

Aqueous Phase Reforming of Industrially Relevant Sugar Alcohols with Different Chiralities

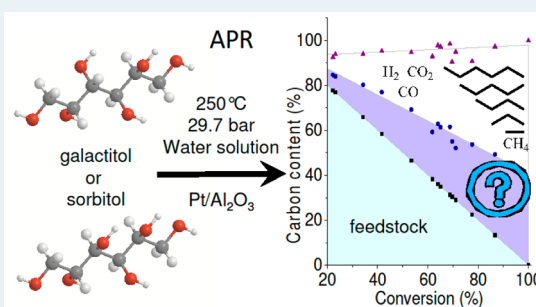
Lidia I. Godina, Alexey V. Kirilin,[†] Anton V. Tokarev, and Dmitry Yu. Murzin*

Laboratory of Industrial Chemistry and Reaction Engineering, Process Chemistry Centre, Åbo Akademi University, FI-20500 Turku, Finland

Supporting Information

ABSTRACT: The influence of substrate chirality was studied in the aqueous phase reforming (APR) over Pt/Al₂O₃ in a continuous fixed-bed reactor at 225 °C. Two epimeric sugar alcohols, namely sorbitol and galactitol, were used for performance comparison. For the very first time galactitol was used in the APR process. The reliability of the liquid-phase product analysis was considerably improved due to application of a spiking technique for qualitative analysis and subsequent peak fitting for quantification. A detailed analysis of the gas and liquid phases showed almost the same behavior of both polyols, apart from the formation of several intermediate oxygenates. This implies that industrially relevant feedstocks with different chiralities can be efficiently processed in APR, since the chirality of the initial substance does not affect the reaction rate and selectivity to the final products. However, the observed difference in the liquid phase composition should be considered, because the catalyst should be active in the conversion of both polyols and oxygenates. Finally, possible reaction pathways were proposed and discussed from a thermodynamic point of view.

KEYWORDS: aqueous phase reforming, sorbitol, galactitol, Pt/Al₂O₃, thermodynamics



1. INTRODUCTION

Over the past decade the volatility of crude oil prices became one of the main driving forces for fuel production from renewable resources, especially from biomass. The abundance of renewable carbohydrates determines the choice of aqueous phase reforming (APR) as a promising technology, which possesses certain advantages. First, the net effect of this approach to greenhouse emissions is zero, since all CO₂ produced was captured from the atmosphere during the process of carbohydrate formation. A second benefit is that, in comparison with one of the most abundant processes, such as steam reforming, APR allows the reduction of energy consumption needed for hydrogen production.^{1,2} Even if the yields of hydrogen in the steam reforming of sorbitol are practically the same as in the APR (50–60%), the operation temperature is substantially lower in the APR (225 °C and 525–625 °C).³ The third advantage is that water, which is used as a solvent, also acts as a reactant, thus being converted into additional hydrogen via the water-gas shift reaction (WGS).

The method of APR allows one to use a wide range of substrates, with methanol, ethylene glycol, glycerol, xylitol, and sorbitol being mostly studied.^{1,4–6} Sorbitol is currently produced in high amounts from glucose;^{7–13} in addition to that, a large number of recent papers have focused on a direct cellulose conversion to sorbitol.^{14–23} Galactitol could be produced from Siberian larch (*Larix sibirica*) wood. This tree species area covers significant parts of Russia and Canada. The concentration of arabinogalactans is up to 20 wt % in dry wood. The main component

of these polysaccharides is galactose (an average ratio of units of galactose/arabinose/glucuronic acid is about 5.6/1/0.08).²⁴ The other sources for galactitol could be galactoglucmannans, which are found in large quantities in softwood²⁵ and can be recovered in the mechanical pulping process from the waste waters.^{24,26,27}

The influence of substrate chirality on the APR parameters such as selectivity and product distribution has not been properly addressed. Deutsch et al.²⁸ carefully examined an aqueous phase hydrogenolysis (APH) of polyols ranging from C₃ to C₆, except for talitol and iditol, over a Ru/C catalyst. The obtained results are essential for the present study, since the conditions of APH are very similar to those of APR. In this process the reaction rates showed a dependence on chirality but were not affected by the carbon chain length of a reactant. Molecules with erythro sequences of hydroxyl groups, where in the Fischer projection two pairs of the same substituents are located on the same side of two adjacent chiral centers, showed the highest rates in hydrogenolysis due to steric or adsorption phenomena involving the Ru surface. Meanwhile, Liu² reported the same hydrogen production rates for mannitol and sorbitol in the APR. According to the data available in the literature, the influence of chirality on APR of polyols is unclear.

Thus, there is an apparent need to investigate the influence of chirality on the APR of sugar alcohols. A comparative study of

Received: November 27, 2014

Revised: March 20, 2015

Published: April 2, 2015

sorbitol and galactitol was performed in the present work to unravel the potential impact of chirality. Additionally, a thorough analysis of the reaction products was performed in order to establish the foundations for the very complex reaction network. Thermodynamic calculations were performed for various plausible reaction pathways in order to exclude unrealistic, thermodynamically forbidden reactions.

2. EXPERIMENTAL SECTION

2.1. Catalyst. A commercially available catalyst was provided by Sigma–Aldrich. The catalyst has a loading of 1 wt % of Pt deposited on γ -Al₂O₃. The catalyst was compressed into pellets and then crushed and sieved to a 125–250 μ m fraction prior to the experiments.

2.2. Catalyst Characterization. **2.2.1. CO Chemisorption.** The platinum dispersion was evaluated from CO titration by means of a CO pulse chemisorption apparatus (Micromeritics, AutoChem 2900). The following program was used for a catalyst pretreatment prior to analysis: heating from 25 to 50 °C at 10 °C/min in He, dwell for 30 min, gas switch to H₂, heating to 250 °C at a rate of 5 °C/min, dwell for 2 h, followed by flushing for 60 min in He at 250 °C. In the first step a 0.10 g sample was prereduced in a U-shaped quartz tube, while in the second step the surface hydrogen was removed. After this procedure the catalyst was cooled to ambient temperature and titrated by CO pulses (10 vol % CO in He). The Pt/CO stoichiometry was assumed to be 1/1.

2.2.2. Temperature-Programmed Reduction. The 0.12 g catalyst sample was reduced in a U-shaped quartz tube during the TPR by means of the AutoChem 2900 instrument with the following program: heating from room temperature to 700 °C at a rate of 10 °C/min. The reduction was performed by 5% H₂ in Ar; a thermal conductivity detector (TCD) was used to measure the hydrogen uptake.

2.3. APR Experiments. The experimental setup for APR is shown in Figure 1. A stainless-steel reactor was located in a

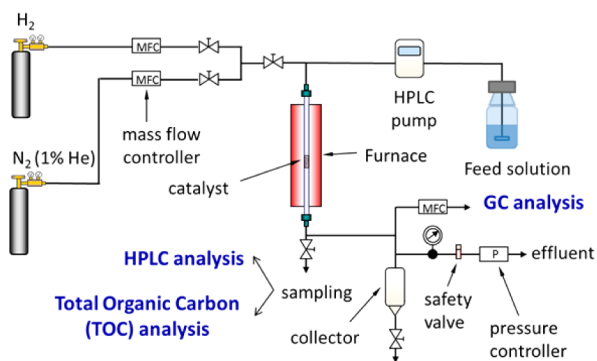


Figure 1. Experimental setup for aqueous phase reforming.

furnace; the catalyst bed was placed in the middle of the reactor between two layers of quartz sand. The polyol solution was fed with an HPLC pump. The reactor was connected to nitrogen (1% He) and hydrogen gas lines. Gas–liquid separation took place in a T-shaped connector with 4 mm inner diameter above a bottle for liquid waste products. There is no need for additional cooling or any extra gas–liquid separation equipment, since constant nitrogen cofeeding during the reaction (flow is 25 mL/min) forms a trickling regime. Liquid samples were periodically taken via a sampling loop for an offline HPLC analysis, while the gas samples were analyzed online by means of Micro-GC.

For all experiments 1.0 g of the fractionized 1% Pt/Al₂O₃ catalyst was used. The experimental studies were done at 225 °C and 29.7 bar. For APR experiments 3.6 wt % water solutions of a substrate were used. The flow rates ranged from 0.1 to 1.0 mL/min, which corresponds to the weight hour space velocities of 0.22–2.16 h⁻¹ calculated as the mass of the substrate per mass of the catalyst per hour ($g_{\text{subst}} g_{\text{cat}}^{-1} h^{-1}$).

In total three experiments were done. In the first and second experiments sorbitol and galactitol solutions (3.6 wt %) were fed within a flow rate range of 0.1–1.0 mL/min, as mentioned above. The experimental sequence of the third experiment is illustrated in Figure 2. Sorbitol solution (3.6 wt %) was fed, followed

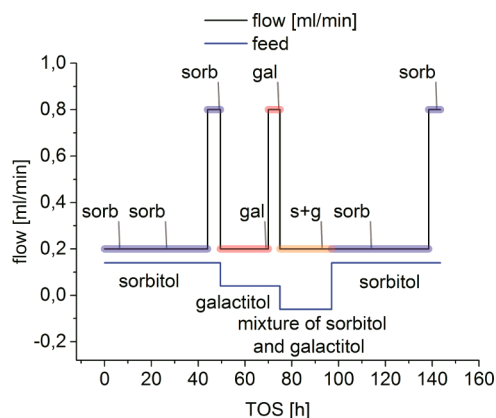


Figure 2. TOS scheme for the sequential experiment, where sorbitol (sorb), galactitol (gal), and a mixture of both polyols (s+g) was fed.

by galactitol solution (3.6 wt %), and then a mixture of polyols (1/1, 3.6 wt % in total) was fed followed by final feeding with sorbitol solution.

The catalyst was reduced in situ prior to all experiments under a hydrogen flow (40 mL/min). The following program was used: heating under a hydrogen flow from room temperature to 250 °C at a rate of 5 °C/min, dwelling for 2 h, cooling to the operating temperature. Residual hydrogen was removed by flushing with N₂ (25 mL/min) for 20 min.

Gas products were quantitatively analyzed online by a micro-GC instrument (Agilent Micro-GC 3000A) equipped with four columns: Plot U, OV-1, Alumina and Molsieve.

The analysis of liquid products was performed by means of an HPLC instrument (Agilent 1100) equipped with an Aminex HPX-87H column, which was quantitatively calibrated for the anticipated reaction products (external standard method). The analysis was performed at 45 °C under isocratic conditions and a flow rate of 0.6 mL/min. The mobile phase consisted of 5 mM H₂SO₄ water solution. The products were analyzed by using a refractive index detector (RI). Peak identification was based on retention times. A total of 89 substances were used in a spiking technique for additional improvement of the confidence of identification. A full list of substances is presented in Table S1 in the Supporting Information. The selection of substances was based on the data reported in refs 29–36. Peak fitting was applied to increase the accuracy of quantification, because of the poor resolution of most peaks, corresponding to polyols and sugars. The fitting procedure was performed with the data-analyzing software OriginPro 9.0.³⁷

A total organic carbon analysis (TOC) was applied to monitor the carbon balance in liquid samples. The observed values were close to 95%.

The following equations were used to calculate the results of experiments.

Conversion of the substrates was determined by

$$\text{conversion (\%)} = \left(1 - \frac{\nu(C_{\text{feedstock}})}{\nu(C_{\text{input}})} \right) \times 100 \quad (1)$$

where $\nu(C_{\text{feedstock}})$ is the molar flow of carbon in the unreacted substrate (mol/min) and $\nu(C_{\text{input}})$ is the molar flow of carbon in the incoming flow of substrate (mol/min).

The results of APR of sorbitol and galactitol were compared on the basis of selectivity to the reaction products. For alkanes, CO₂, CO, and products in the liquid phase selectivity was calculated by

$$\text{selectivity to product X (\%)} = \frac{\nu(C_x)}{\nu(C_{\text{gas}})} \times 100 \quad (2)$$

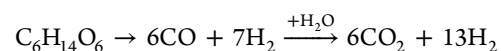
where $\nu(C_x)$ is the molar flow of carbon, contained in a product (mol/min).

The moles of carbon in a product is determined as

$$\nu(C_x) = C_x v n \quad (3)$$

where C_x is the molar flow of the product (mol/(L min)), ν is the volumetric flow (L/min), and n is the number of carbon atoms in a product.

The additional parameter “reforming ratio”, RR (H₂/CO₂), was introduced to calculate the selectivity to hydrogen, since hydrogen is produced both from polyols and via the water-gas shift (WGS) reaction:



Selectivity to hydrogen is defined by

$$\text{selectivity to H}_2 \text{ (\%)} = \frac{\nu(H_2)}{\nu(C_{\text{gas}})} \frac{1}{RR} \times 100 \quad (4)$$

where $\nu(H_2)$ is the moles of H₂ formed and RR = 13/6 for sorbitol and galactitol.

3. RESULTS AND DISCUSSION

3.1. Catalyst Characterization. The commercial catalyst 1% Pt/Al₂O₃ was completely reduced prior to APR experiments, as evidenced by a corresponding TPR profile in Figure 3. The

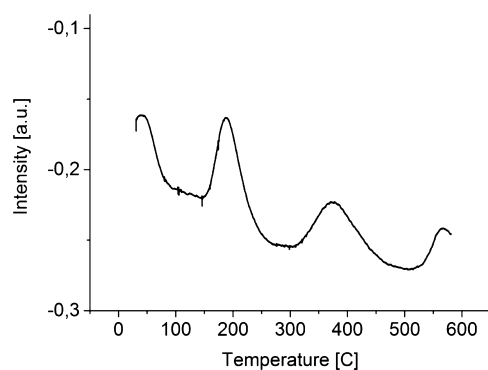


Figure 3. TPR profile of Pt/Al₂O₃ catalyst.

reduction peak of the surface PtO₂ species, weakly interacting with the support, starts at 39 °C. Reduction of Pt oxides interacting with Al₂O₃ occurs more strongly at 188 °C. A high-temperature peak observed at 372 °C can be assigned to the

formation of a PtO₂–Al₂O₃ complex.³⁸ The reduction of the support occurred at temperatures above 580 °C due to interactions between Pt and Al₂O₃ and formation of Pt–Al alloy.³⁹

The surface properties of the catalyst were elucidated by means of pulse CO chemisorption. The Pt/Al₂O₃ catalyst has a metal dispersion of 52% with a metallic surface area of 129 m²/g of metal and an average particle diameter of 2.2 nm.

3.2. Test of Polyols. **3.2.1. Conversion of Substrate and Carbon Distribution between Phases.** Previously, similar types of catalysts were used for the APR of various polyols,^{29,40–50} despite the concern that a support such as Al₂O₃ can be transformed into boehmite under experimental conditions. Copeland et al. demonstrated that alumina support is reasonably stable in the presence of a polyol such as glycerol, even on testing in overheated water.⁴¹ This observation contradicts with XRD data obtained by Doukkali et al.⁵¹ Severe transformations of Pt/Al₂O₃ were confirmed for the same reaction due to incorporation of water molecules in the catalyst matrix.⁵¹ Similar conditions were applied in the current work. However, support alteration could be a slow and time-dependent process. The duration of experiments probably plays a crucial role. According to Figures 4 and 5,

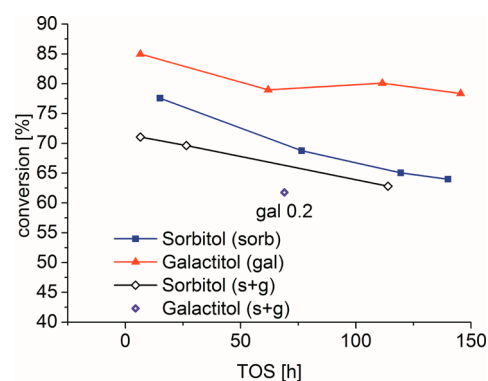


Figure 4. Performance of 1% Pt/Al₂O₃ catalyst as a function of time on stream (TOS) at 225 °C, 29.7 bar, and flow rate 0.2 mL/min: conversion of the substrates. Abbreviations: sorb, the experiment with sorbitol only; gal, the experiment with galactitol; s+g, sequential experiment with both polyols (see section 2.3).

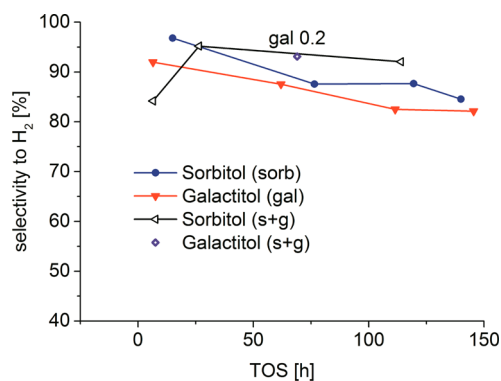


Figure 5. Performance of 1% Pt/Al₂O₃ catalyst as a function of time on stream (TOS) at 225 °C and flow rate 0.2 mL/min: selectivity to H₂. Abbreviations: sorb, the experiment with sorbitol only; gal, the experiment with galactitol; s+g, sequential experiment with both polyols (see section 2.3).

no significant deactivation was observed during 135 h of time on stream for the whole experimental program. The conversion

level, as well as selectivity to hydrogen, decreased slightly during the first 20 h due to the initial deactivation.

Figure 6 displays conversion dependence on weight hour space velocity (WHSV) for all three experiments with sorbitol,

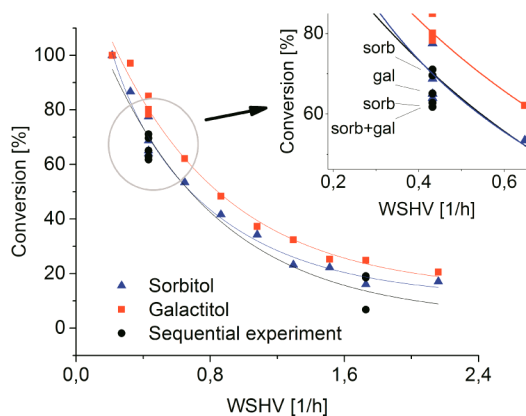


Figure 6. Conversion of the substrate as a function of WHSV for sorbitol and galactitol at 225 °C and 29.7 bar. Abbreviations: sorb, the experiment with sorbitol only; gal, the experiment with galactitol; s+g, sequential experiment with both polyols (see section 2.3).

galactitol, and the mixture thereof. Conversion levels varied from 15 to 100%. A small discrepancy between the conversion levels of sorbitol and galactitol is clearly visible in Figures 4 and 6. This difference can be attributed to probable differences in the catalyst wetting, rather than the properties of the substances. This hypothesis was supported by the results of the third sequential experiment (see insert in Figure 6), which gave exactly the same levels of conversion for both polyols and their 1/1 mixture.

The distribution of carbon during APR experiments was studied by means of TOC along with the analysis of the gas phase composition; the results for sorbitol are shown in Figure 7a. The

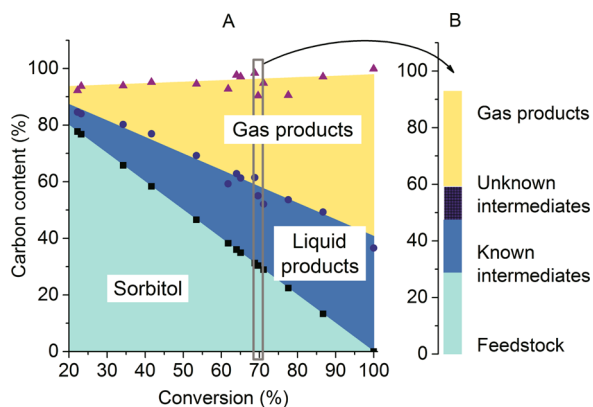


Figure 7. Carbon distribution between the liquid and gas phases and total carbon balance versus conversion in APR of sorbitol at 225 °C and 29.7 bar: (a) the whole conversion region; (b) carbon distribution at 62% conversion.

mass balance on the basis of the carbon content observed is shown as an upper segment of the diagram, being close to 95% in both experiments. The distributions of carbon between the gas and the liquid products were found to be very similar for both sugar alcohols. Remarkably, almost 42% carbon (fed to the reactor in the form of polyol) is still present in the liquid phase in

the form of oxygenated products, whereas conversion of the initial substrate already reached 100%.

3.2.2. Selectivity to Gas-Phase Products. The selectivity to the gas phase products was calculated according to eqs 2 and 4. The results obtained are provided in Figures 8 and 9. It was found

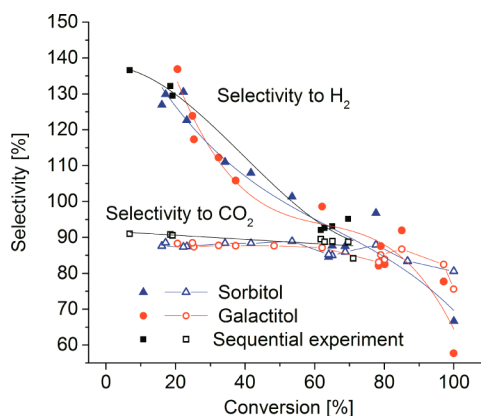


Figure 8. Selectivity to H₂ and CO₂ versus carbon conversion in the APR of sorbitol and galactitol at 225 °C and 29.7 bar.

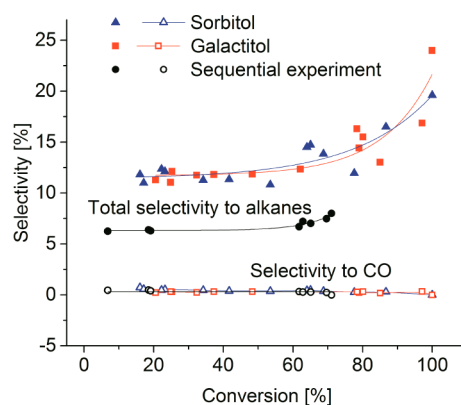


Figure 9. Selectivity to CO and alkanes versus carbon conversion in the APR of sorbitol and galactitol at 225 °C and 29.7 bar.

that the selectivities to some gaseous products (H₂, CO, and CO₂) were similar for both polyols over the whole range of substrate conversion (20–100%). Selectivity to hydrogen decreased significantly with an increase in conversion due to consumption of hydrogen in hydrogenation reactions, in contrast to a rapid growth of the total selectivity to alkanes. The last parameter is much lower in comparison to hydrogen selectivity (see Figure 7), as was already shown by Kirilin et al.²⁹ The selectivity to CO was close to 0, indicating that almost all carbon monoxide was converted to CO₂ via the water-gas shift reaction (WGS) under experimental conditions, as demonstrated by Haruta and co-workers.⁵² It is noteworthy that selectivity to alkanes appeared to be slightly different in the sequential experiment, which probably happened due to minor changes in the equipment with time. The sensitivity to alkanes changed between the first two experiments (sorbitol and galactitol) and the the third experiment (sequential experiment). However, all data points from the sequential experiment lay in a row, indicating the same selectivity in the case of both polyols and their mixture.

A detailed comparison of alkanes is provided in Figures 10 and 11. The selectivities to alkanes for both substrates were identical, showing no effect of chirality on this parameter (see the

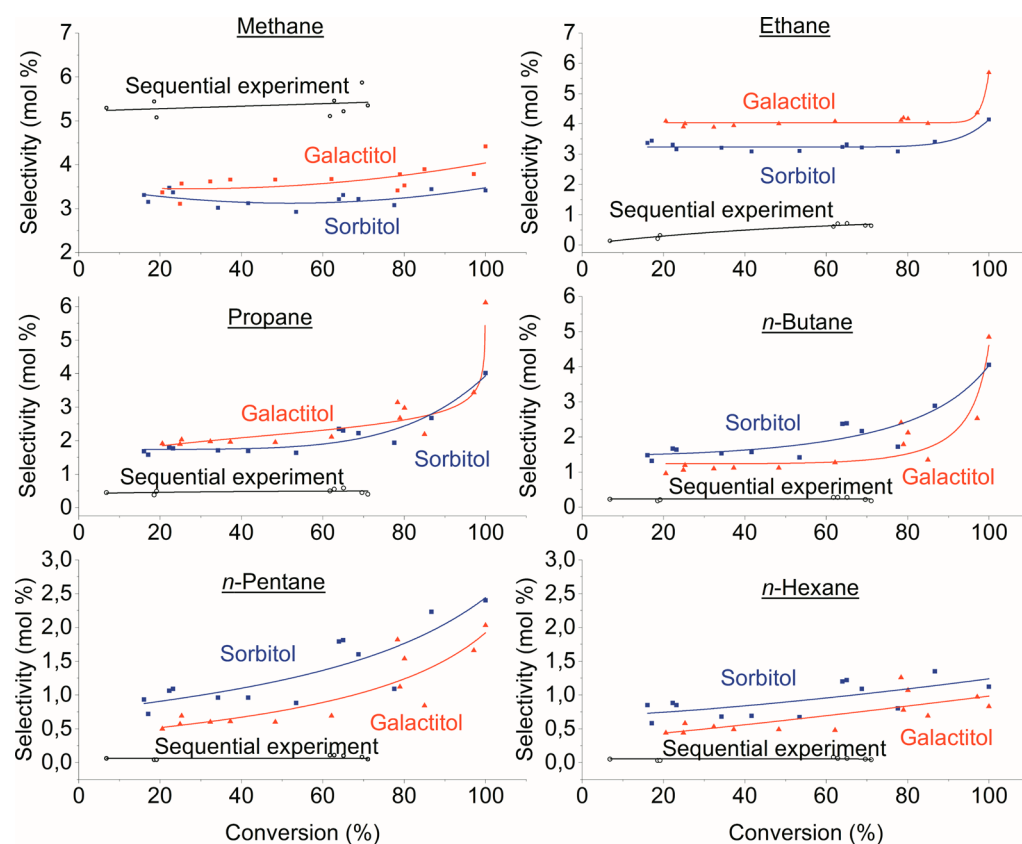


Figure 10. Selectivity to linear alkanes versus carbon conversion in the APR of sorbitol and galactitol at 225 °C and 29.7 bar.

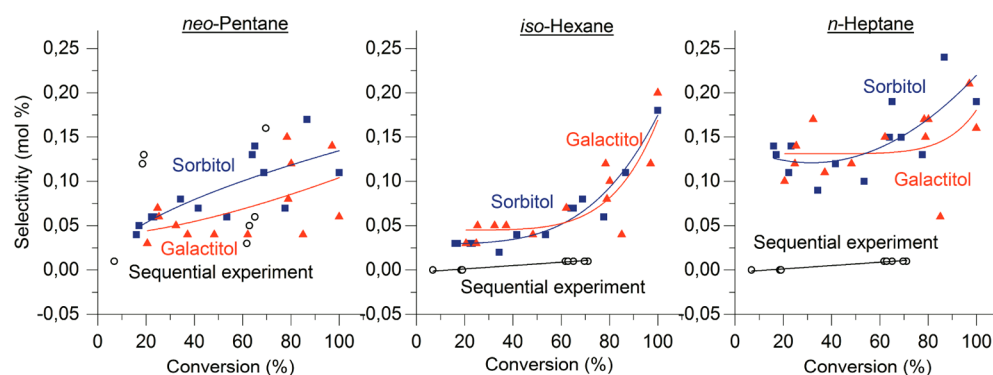


Figure 11. Selectivity to branched alkanes and heptane versus carbon conversion in the APR of sorbitol and galactitol at 225 °C and 29.7 bar.

sequential experiment). The discrepancy between different experiments is explained above. For all hydrocarbons, the selectivity increases with conversion. It is noteworthy that some amounts of branched pentane and isohexane were detected in the gas phase, indicating some skeletal isomerization process during APR. However, isobutane or unsaturated compounds were not observed. Traces of heptane were also found, although it contains more carbon atoms than the starting C_6 -polyol. However, for the concentrations of heptane detected, some variation in experimental data was observed (Figure 11), which might be caused by the limited volatility of hydrocarbons heavier than pentane at room temperature and atmospheric pressure.

3.2.3. Selectivity to Liquid-Phase Products. In-depth studies of liquid-phase composition during polyol conversion were performed mainly for aqueous-phase dehydration/hydrogenation (APD/H) on Pt/ Al_2O_3 - SiO_2 ,^{30,31} Pt/ TiO_2 + ZrO_2 - WO_x ,^{32,33} Ru/C, and Re-Ru/C.³⁴ Oxygenates were analyzed in the APR of

sorbitol on Ni and bimetallic Ni-Pd catalysts supported on Al_2O_3 , ZrO_2 , and CeO_2 ,³⁵ as well as Pt/ Al_2O_3 .²⁹ The identification of oxygenates was mostly based on direct HPLC analysis or a combination of HPLC with GC-MS. In the work of Kirilin et al. analysis of intermediates in the APR of sorbitol on Pt/ Al_2O_3 also involved solid-phase microextraction.³⁶ More than 250 intermediates with 50 major compounds were detected.

In the present study the composition of the liquid phase was thoroughly elucidated by means of HPLC, which allowed identifying approximately 62% of the carbon stored in all intermediates. The distribution of identified and unknown carbon is shown at 68% conversion of sorbitol in Figure 7b. Considering that all gaseous carbon was identified, one can conclude that approximately 80% of the carbon is accounted for among the known substances.

The selectivity to identified liquid products was calculated according to eqs 2 and 3. The results obtained in the current

Table 1. Selectivity to Substances Found in the Liquid Phase during the APR of Sorbitol and Galactitol and APDH of Sorbitol

substance	selectivity (mol % C)				
	galactitol ^a	sorbitol ^b	ref 47 ^c	ref 31 ^d	ref 45 ^e
Alcohols					
2-methylcyclopentanol			trace ^f		
2-methylpentanol			trace		
butane-1,2-diol	0.47	0.64	trace		
butane-1,2,4-triol			trace		
butane-2,3-diol	0 ^g	0	0	0.70	0
butan-1-ol	0	0	trace		0.50
butan-2-ol			trace		
ethanol	2.02	3.02	1.46	0.60	2.10
ethylene glycol	0	0	trace		
glycerol	1.36	1.75			4.00
hexane-1,2-diol	0.10	0.09	trace		1.40
hexane-1,2,6-triol	0	0	trace		0
hexane-2,5-diol	0.18	0.19			
hexan-1-ol	0	0	7.02	2.40	1.10
hexan-2-ol	0	0	trace		
hexan-3-ol	0	0	trace		
propan-2-ol	0	0	trace		
methanol	6.96	5.20	trace	0.30	0.40
pentane-1,2-diol	0	0	trace	0	7.80
pentan-1-ol	0.06	0.06	9.50	3.70	0.30
pentan-2-ol	0.04	0.02	trace		
propane-1,2-diol	1.39	1.35	trace		3.60
propan-1-ol	1.45	1.74	trace	1.10	1.10
Acids					
acetic acid	0.54	0.82	0		
butyric acid	0	0	0	2.80	
fumaric acid	0	0.69			
hexanoic acid	0.07	0.04	trace	0	
lactic acid	0.15	0.10			
pentanoic acid	0	0	trace		
propanoic acid	0	0	trace		
pyruvic acid	1.71	0.08			
tartaric acid	0	0.03			
Aldehydes/Ketones					
3-hydroxy-2-butanone	1.49	1.59			
3,4-hexanedione			trace		
acetone	0.53	0.25	trace		0.20
butanone			trace	2.00	0.20
hexan-3-one	0	0	10.53	6.30	1.10
hexan-2-one			10.53		
pentane-2,3-dione	0	0	trace		
pentanone			trace	2.00	0.20
pentan-3-one			4.39		
Furans/Pyrans					
2-acetylfuran	0.02	0.02			
2-methyltetrahydrofuran	0	0	trace	5.90	0.50
2-methyltetrahydropyran			trace	5.00	0.30
2,4-dimethyltetrahydrofuran			trace		
2,5-dimethyltetrahydrofuran	0.06	0.04	trace	5.30	0.60
5-hydroxymethyl-2-furaldehyde	0.06	0.07			
tetrahydrofuran			trace	1.00	0
tetrahydrofurfuryl alcohol	0.45	0.17		43.00	2.90
tetrahydropyran	0	0		1.20	0.30
tetrahydropyran-2-methanol	0	0	trace	13.70	6.20
Sugars and Sugar Alcohols					
1,4-sorbitan			185.96	78.50	27.00
D-(+)-arabitol	0.56	0.15			
D-(+)-glucose	0.003	0.11			

Table 1. continued

substance	selectivity (mol % C)				
	galactitol ^a	sorbitol ^b	ref 47 ^c	ref 31 ^d	ref 45 ^e
	Sugars and Sugar Alcohols				
D-galactose	0.10	0			
D-sorbitol	0	14.06	74.56		
galactitol	15.79	0			
isosorbide	0	0	54.39	20.50	27.00
meso-erythritol	1.12	0.95			
xylitol	0.99	1.05			

^aAPR of galactitol over 1% Pt/Al₂O₃ at 225 °C, 29.7 bar, and 65% conversion. ^bAPR of sorbitol over 1% Pt/Al₂O₃ at 225 °C, 29.7 bar, and 62% conversion. ^cAPDH of sorbitol over 2.2% Pt/ZrO₂+TiO₂-WO_x (20/80) at 220 °C, 22 bar, and 91.5% conversion. ^dAPDH of sorbitol over 4% Pt/zirconia phosphate at 245 °C, 26.1 bar, and 58% conversion. ^eAPDH of sorbitol over 4% Pt/Al₂O₃-SiO₂ at 225 °C, 29.3 bar, and 74.6% conversion. ^fTrace indicates that the compound is detected, but its amount is lower than 0.005 mol/mol of sorbitol converted. ^gZero entries indicate that a substance concentration is below the sensitivity of the RI detector (the detection limit strongly depends on the type of substance and can be in the range 8–800 mmol/L, assuming a signal-to-noise ratio (S/N) of 3).

study are combined with the results from the previous studies on the APDH of sorbitol over different catalysts^{30–32} and are shown in Table 1. However, the concentration of some substances was lower than the detection limit; therefore, those species were not inserted in Table 1 (the full list of compounds is provided in Table S1 in the Supporting Information). It should be also noted that the denominator in eq 2 contains the amount of carbon in the gas phase, which means that the selectivity could exceed 100%, if carbon remains mostly in the liquid phase.

The composition of the liquid phase in the current study can be easily obtained from Table 1, since the selectivity values are shown for very close levels of conversion: 62 and 65% for sorbitol and galactitol, respectively. The product distributions are very similar for the samples obtained during APR of both polyols; in both cases similar sugars, polyols, alcohols, acids, carbonyl compounds, and furans were found. One notable exception is the presence of distinct primary intermediates, such as glucose and galactose. No galactose was found in the sample from sorbitol, and only traces of glucose appeared in the sample from galactitol. However, this method does not give a good separation of sugars and sugar alcohols; therefore, only substances with high concentration can be taken into account. Interestingly, even though the selectivity to arabitol was also significantly higher in the case of galactitol, xylitol was also found among the products, indicating that diastereomerization reaction can take place. It is worth noting that such substances as tartaric and fumaric acids (2,3-dihydroxybutenedioic and 2-butenedioic acids, respectively) were found as the products of sorbitol conversion, but not in the case of galactitol.

A comparison with APDH data, when additional hydrogen was supplied, revealed higher selectivity to alcohols with a longer chain (hexanol, pentanol) and lower selectivity to methanol and ethanol. It could be assumed that additional hydrogen would increase the total amount of hydrogenolysis reactions of the C–O bond, preventing C–C bond cleavage. All catalysts used for APDH were prepared using supports with acidic properties, which influenced the reaction pathways and resulted in higher concentrations of cyclic products in comparison to APR. The polyol transformation started from the formation of cyclic 1,4-sorbitan and isosorbide, which were found to be the main intermediates at early stages of the APDH reaction. This leads to significantly higher selectivity to heterocyclic compounds, such as furanic or pyranic compounds. At the same time, isosorbide was not found during APR of sorbitol or galactitol, although the conversion level was close to 60%.

Identification of isosorbide could be obstructed due to the presence of glycerol among the reaction products, which should be taken into account. The retention times of isosorbide and glycerol are very close, which can be easily seen in Figure 12,

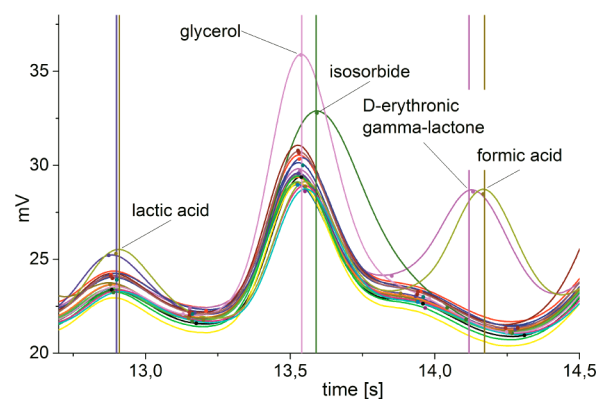


Figure 12. Glycerol and isosorbide peaks in the galactitol sample.

presenting a part of the HPLC chromatogram with 19 curves. Every curve represents the same liquid sample obtained during the APR of galactitol, which was mixed with a solution of some substances, given in Table 1. The purple curve represents the sample with glycerol addition, while the green curve corresponds to isosorbide addition; the others do not contain any of these substances. Therefore, the peak with a retention time of about 13.51 min can be assigned with a high level of certainty to glycerol.

A comparison with APDH data revealed similar values of selectivity to some products. Nevertheless, additional experiments are needed to evaluate the influence of additional hydrogen on the liquid-phase products.

3.2.4. Influence of Stereoselectivity and Possible Reaction Pathways. A certain number of sugar alcohols can be produced from plant biomass. They can differ in the chain length and in chirality. An increase in the carbon chain length implies an increase in the number of possible stereoisomers: two for tetraols, three for pentaols, and six for hexitols. These stereoisomers differ in their internal bonds, which sometimes has a profound influence on their properties. The solubility of galactitol in water can serve as a good example, being approximately 20 times lower than the solubility of sorbitol at temperatures between 15 and 100 °C (see Figure 13).⁵³ The

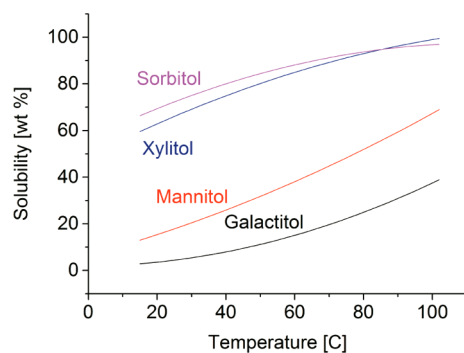


Figure 13. Solubility of alditols according to the Kroschwitz and Howe-Grant equation.⁵³

differences in properties of these stereoisomers can be attributed to conformational differences in chirality of these molecules. Sorbitol has a strong 1,3-nonbonded interaction between C₂ and C₄ hydroxyl groups, being in a zigzag conformation, which destabilizes it by 6.28 kJ/mol, and four 1,3-*syn*-axial interactions (two between C₃ oxygen and C₁ and C₅ hydrogens and one between C₅ oxygen and C₆ hydrogen), which additionally

destabilize this conformation by 7.53 kJ/mol.⁵⁴ As a result, D-sorbitol exists in water solution and in the crystalline state predominantly in a sickle (bent) conformation, while D-galactitol retains the zigzag conformation. Even if these minor differences could be anticipated to have much influence on the APR process performed at 225 °C, they made a significant difference in hydrogenolysis studied at 205–240 °C.²⁸ Assuming high similarities between APDH and APR processes, it can be concluded that Pt and Ru catalysts behave differently.

As is shown in Figures 8–11 and Table 1, the chirality of substrates does not have a considerable influence on the selectivity to the final products or to the intermediates to a large extent, which is an advantage for an industrial process, where the feedstock can be a mixture of isomers. However, there is a notable difference between sorbitol and galactitol behaviors at early stages of the APR reaction, when dehydrogenation of the substrate leads to the formation of sugars: galactose from galactitol and glucose from sorbitol, respectively.

The scheme of the main reaction pathways, which is based on the product analysis, is displayed in Figure 14. The substrate is C₆-polyol, which can be transformed into C₅-polyol via consecutive dehydrogenation/decarbonylation steps (steps 1 and 2)

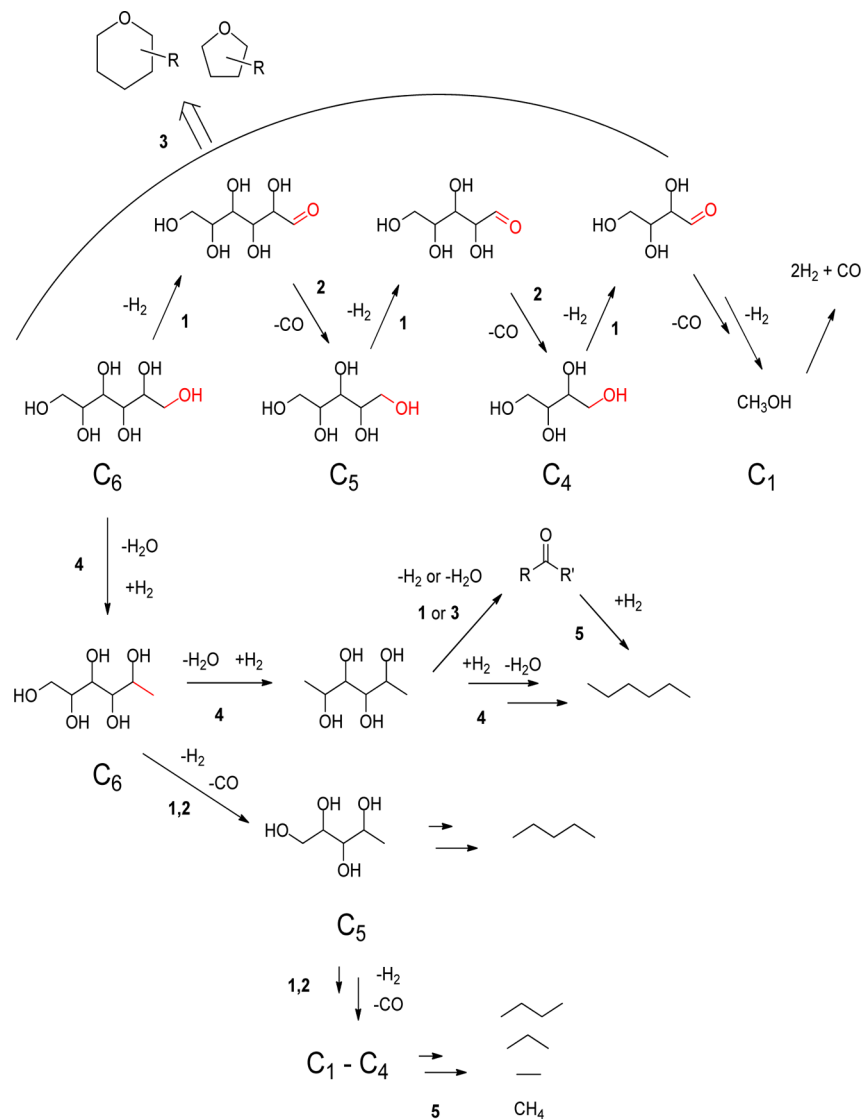


Figure 14. Main reaction pathways in the APR of sorbitol and galactitol.

occurring on the metal sites.^{30,47,55} Subsequent repetitions of these steps result in a complete conversion of the substrate to CO and hydrogen. On Pt/Al₂O₃ almost all CO reacts with water to form CO₂ and additional H₂ via the WGS reaction. Intermediate aldols can desorb from the surface. Aldehydes C₄–C₆ can be transformed into stable cyclic products (substituted tetrahydrofurans and tetrahydropyrans) via dehydration (step 3) occurring on acidic sites. Hydrogenolysis of primary hydroxyl groups (step 4) gives molecules with a nonreactive methyl group at the end and less reactive secondary hydroxyl groups. These secondary alcohols are either transformed into ketones via dehydrogenation (step 1) or dehydration (step 3) or undergo complete reduction to form alkanes (step 5), depending on the conditions. Since Pt favors dehydrogenation and C–C bond breaking, the main alkanes produced will be alkanes with low molar mass: ethane and propane. Desorbed aldehydes are easily converted into *gem*-diols, which can be dehydrogenated on Pt with the formation of acids (see Figure 15).^{50,56–59} Aldol

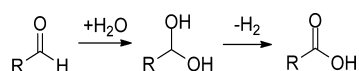


Figure 15. Formation of acids from aldehydes via *gem*-diol dehydrogenation.

condensation is also preferred to Cannizzaro disproportionation, when the reacting aldehyde contains an α -hydrogen atom.⁶⁰

All possible optically active hexoses and pentaols formed starting from D-galactitol and D-sorbitol are shown in Figure 16,

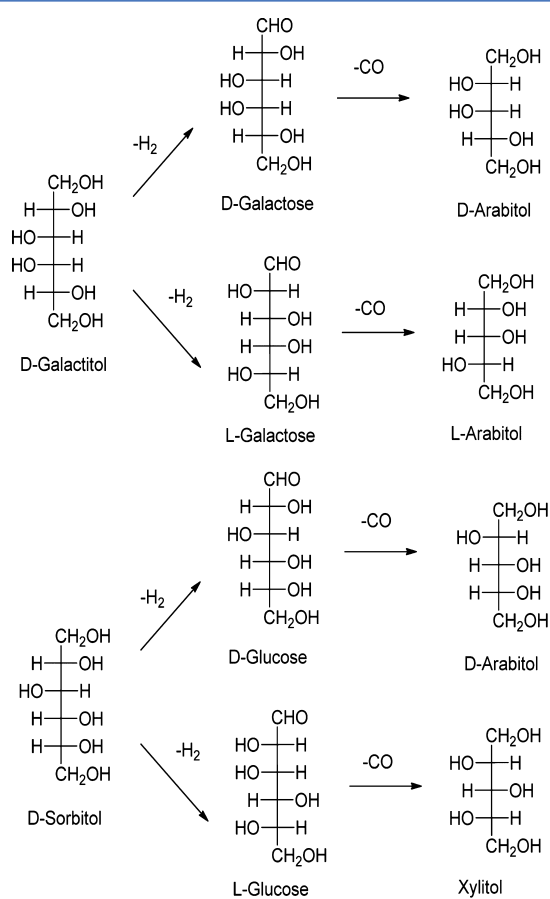


Figure 16. Galactitol and sorbitol dehydration/decarbonylation in the APR.

assuming that only steps 1 and 2 take place. Neither glucose nor xylitol can be produced from galactitol via this path; however, they were found in small amounts among the liquid-phase products. Transition metals such as Au, Pd, and Ru are known to catalyze the racemization of alcohols, being used as a heterogeneous catalyst in dynamic kinetic resolution in combination with enzymes.^{61–63} However, Pt itself was not as widely applied, probably due to interactions with enzymes.^{64,65} Thus, one can tentatively assume that diastereomerization also takes place during the APR (see Figure 17).

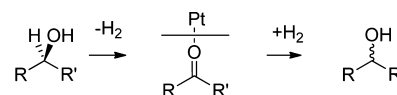


Figure 17. Diastereomerization of carbohydrates on Pt surface via dehydrogenation/hydrogenation steps.

At 225 °C and 30 bar the ionization constant of water⁶⁶ is $K_w = 5.597 \times 10^{-12}$, corresponding to pH 5.628, which can promote reactions requiring protonation steps. Typically, heterogeneous catalytic isomerization of alkanes requires strong acidity, thus demanding another explanation for branched alkane formation. Pinacol–pinacolone rearrangement of desorbed aldehydes can be a plausible explanation for branching (see Figure 18).

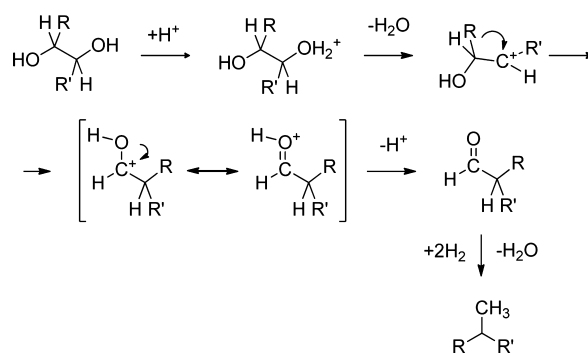


Figure 18. Pinacol–pinacolone rearrangement with subsequent reduction to branched alkane.

Despite the fact that a retro-aldol reaction was assumed in many papers to be one of the possible reaction paths, no clear evidence has been presented in the literature and in the current study for the presence of this reaction during the APR process on Al₂O₃- or carbon-based catalysts. This reaction requires some specific conditions, as a special type of support or addition of a basic promoter. A base-catalyzed retro-aldol reaction allowed production of significant amounts of glycerol from sorbitol and both glycerol and ethylene glycol from xylitol during hydrogenolysis on Pt/NaY zeolite⁶⁷ or in the presence of Ca(OH)₂.^{68–70} It should be noted that two molecules of glycerol can be formed from sorbitol only through transformations to keto-hexose, but not aldohexose. However, transformation of the aldehyde form to the keto form should occur rather easily. Therefore, the exact mechanism of dehydrogenation is still unclear. The distribution of gas and liquid products in our experiments does not confirm that a retro-aldol reaction plays a significant role in APR transformations. However, this reaction is thermodynamically possible, as described below.

Secondary alcohols with unsubstituted neighboring atoms do not undergo C–C bond cleavage, which was nicely shown by Vilcoq et al.³²

As mentioned above, one of the unexpected products was *n*-heptane, which contains one more carbon atom than the substrate. The formation of hexane was detected by Jiang et al.⁷¹ during the APR of xylitol over Pt/HZSM-5 and Ni/HZSM-5 catalysts. This fact was explained by ketone formation from xylitol with subsequent aldol condensation and hydrodeoxygenation; another explanation was based on a Fischer–Tropsch synthesis. It should be noted that only branched alkanes could be produced after aldol condensation of ketones, while the authors did not mention if they observed linear or branched hexane. No Fischer–Tropsch synthesis occurs during the APR, which was proven by additional tests of the complementary water-gas shift reaction, where the relationship between the APR and the WGS was thoroughly studied.^{72–74} Thus, the formation of compounds with longer carbon chains could be a result of a sequence of condensation reactions. A possible pathway is illustrated in Figure 19, showing a reversible aldol and subsequent croton

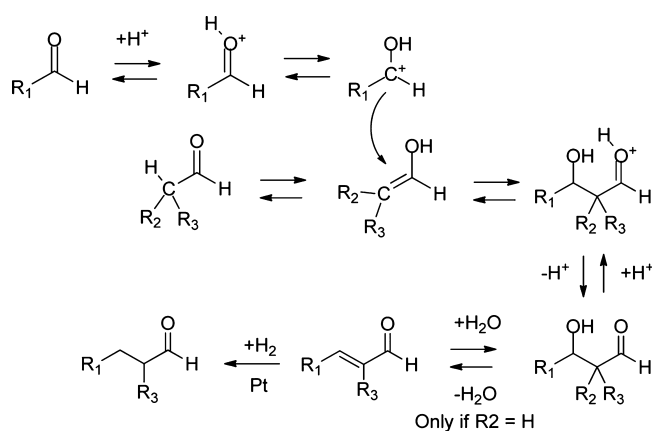


Figure 19. Extension of a carbon chain via aldol and croton condensation and retro-aldol reaction.

condensations. This process is reversible, and under these experimental conditions a retro-aldol reaction can occur as well. Branched alkanes were not previously detected for the APR process over Pt/Al₂O₃; however, an addition of a solid acid such as SiO₂-Al₂O₃ promoted the formation of about 5% of branched alkanes⁷⁵ to achieve a total selectivity of up to 5%. Substantial quantities of isoparaffins were observed for the APR of sorbitol over Ni/HZSM-5 catalyst.^{76,77}

3.3. Thermodynamic Aspects. Changes in standard Gibbs energy in the conversion of glycerol to different intermediates with the same chain length and in the conversion of acetone to liquid fuels were nicely demonstrated by Simonetti and Dumesic.⁷⁸ Aqueous and vapor phase reforming of ethylene glycol has been discussed by Kandoi et al.⁷⁹ Thermodynamic analysis and Gibbs energy minimization was performed for the APR of methanol, acetic acid and ethylene glycol,⁸⁰ glycerol,⁸¹ polyols,⁸² and C₆ compounds.⁸³ These calculations were performed to reveal the thermodynamic feasibility of a number of reactions, which could be a part of a complex APR network.

A reaction is considered to be thermodynamically favorable if the free Gibbs energy of the reaction is below zero: $\Delta G^\circ_r < 0$. Direct calculation of all possible ΔG°_r values for each possible reaction is challenging, due to the huge number of possible reactants. Meanwhile, some values will be helpful to elucidate the overall reaction network. In most cases several examples are presented for the same reaction types (Table 2).

Gas-phase thermodynamic properties of some reactants and products were calculated using HSC Chemistry 6.0,⁸⁴ which has an extensive database but does not cover many of the reactants involved in the APR. The properties of those compounds were estimated via HyperChem 8.0 molecular modeling software,⁸⁵ using the semiempirical quantum-mechanical method PM3. Free Gibbs energies of formation $\Delta G^\circ_f(498\text{ K})$ of some compounds are provided in the Supporting Information. In some cases the values calculated in HCS 7 are provided for a liquid (l) or aqueous (aq) phases instead of a gas phase (g). Gibbs formation energies, which were estimated in the HyperChem software, should be taken into account as approximate values for such substances as glyceraldehyde, aldotetrose, aldopentose, aldohexose, and ketohexoses and polyols such as tetraol, pentitol, and hexitol. The reason is that, even if geometry optimization was performed, the values could differ for different optical isomers.

In most cases Gibbs energies calculated using HCS 7 differ from the HyperChem values, except for hydrogenolysis and dehydration reactions. Despite these differences, the values which were estimated in HyperChem follow the same trends.

Gibbs energies for the most meaningful reactions are shown in Table 2 and discussed below.

Methanation of CO is thermodynamically favorable (-96.66 kJ/mol). However, it was demonstrated that methanation does not occur under the experimental conditions of APR on Pt, Re, Rh, PtRe, and RhRe catalysts supported on Al₂O₃ or carbon.^{74,86,87} Thus, methane formation in the current case mostly happens via C–C bond breaking in acetaldehyde.

The presence of a thermodynamically favorable (-20.5 kJ/mol) water-gas shift reaction was also proven under APR conditions.^{74,86,87}

The Gibbs energies were calculated for the reduction of the carbonyl group. A reversed reaction of dehydrogenation is shown as path 1 in Figure 14. Dehydrogenation is proposed to be the first step of the APR mechanism. However, reduction was found to be even slightly favorable for sugars according to HCS 7 calculations (-15.86 kJ/mol for reduction of glucose to sorbitol). For shorter molecules, such as aldopentoses and glyceraldehyde, the values should be very similar, in accordance with HyperChem values. Reduction of ethanedial to 1,2-propanediol is also thermodynamically favorable (-71.63 kJ/mol). Hydrogenation is slightly favorable for unsubstituted molecules such as hexanal and propionaldehyde (close to -10 kJ/mol). The case with ketones is the opposite: reduction of acetone and hexanones is unfavorable ($3–4$ kJ/mol). At an elevated temperature, such as $200–250$ °C, the reaction should be predominantly under thermodynamic control. Therefore, the reduction of aldehydes should prevail over the reduction of ketones. This leads to the idea that the reverse reaction of dehydrogenation of secondary hydroxyl groups should dominate over dehydrogenation of primary group, unlike what is proposed in section 3.2.4. However, the Gibbs energy values are close to 0; thus, the equilibrium constant should be close to 1, and various hydrogenation/dehydrogenation reactions should take place in this system.

Carbon monoxide is proposed to be formed also by decarbonylation of aldehydes (path 2 in Figure 14). This assumption is in line with the Gibbs energies. Decarbonylation of sugars and glyceraldehyde should be thermodynamically favorable according to HyperChem estimations (from -69 to -77 kJ/mol). The values calculated in HSC 7 are contradictory, due to insufficient information in the database. Decarbonylation of unsubstituted compounds such as hexanal, propionaldehyde,

Table 2. Calculated Free Gibbs Energy of Possible Reactions during APR of C₆ Sugar Alcohols at 498 K^a

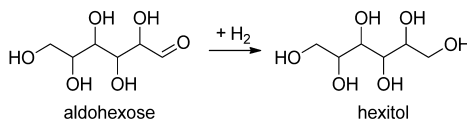
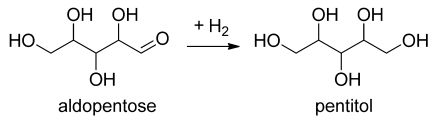
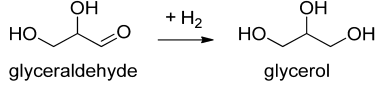
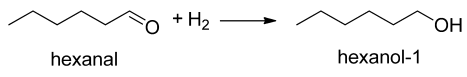
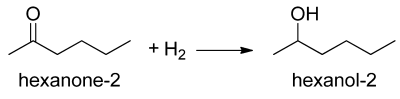
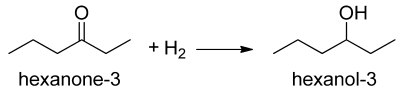
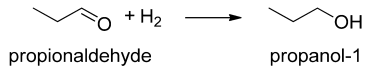
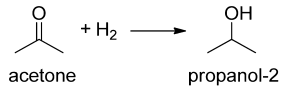
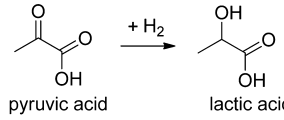
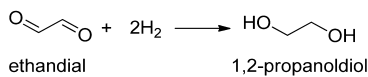
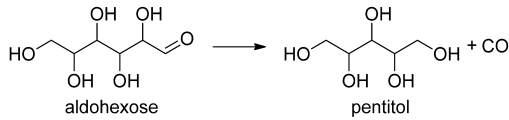
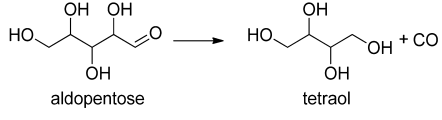
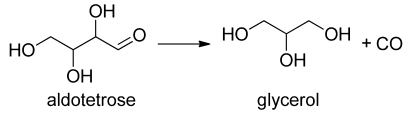
Reaction	Comment	HyperChem $\Delta G^{\circ}f$ (498 K) kJ/mol	HSC7 $\Delta G^{\circ}f$ (498 K) kJ/mol
Reduction of carbonyl group			
 <p>aldohexose $\xrightarrow{+H_2}$ hexitol</p>		14.69	-15.86
 <p>aldopentose $\xrightarrow{+H_2}$ pentitol</p>	*, **	18.66	90.42
 <p>glycerinaldehyde $\xrightarrow{+H_2}$ glycerol</p>	*	7.91	-63.64
 <p>hexanal $\xrightarrow{+H_2}$ hexanol-1</p>		21.84	-10.13
 <p>hexanone-2 $\xrightarrow{+H_2}$ hexanol-2</p>		34.14	3.77
 <p>hexanone-3 $\xrightarrow{+H_2}$ hexanol-3</p>		21.74	3.48
 <p>propionaldehyde $\xrightarrow{+H_2}$ propanol-1</p>		10.67	-9.20
 <p>acetone $\xrightarrow{+H_2}$ propanol-2</p>		-	2.68
 <p>pyruvic acid $\xrightarrow{+H_2}$ lactic acid</p>		-	47.53
 <p>ethandial $\xrightarrow{+2H_2}$ 1,2-propanediol</p>		-	-71.63
Decarbonylation			
 <p>aldohexose \rightarrow pentitol + CO</p>	*	-66.73	48.20
 <p>aldopentose \rightarrow tetraol + CO</p>	**	-69.16	-55.19
 <p>aldotetrose \rightarrow glycerol + CO</p>	*	-77.32	-143.68

Table 2. continued

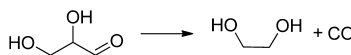

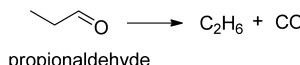
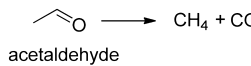
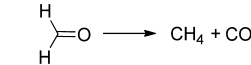
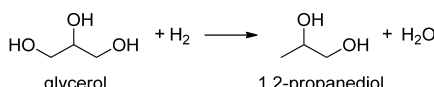

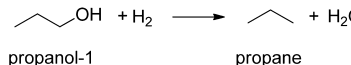
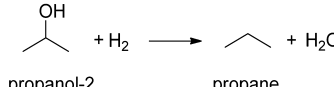
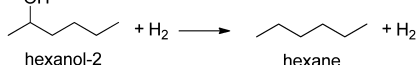
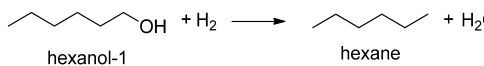
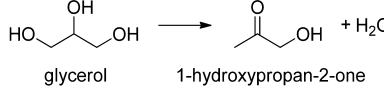
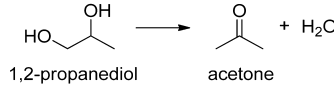
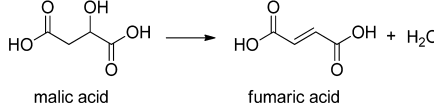

Reaction	Com ment	HyperChem ΔG°_f (498 K) kJ/mol	HSC7 ΔG°_f (498 K) kJ/mol
 glycerinaldehyde \rightarrow 1,2-ethanediol + CO	*	-70.25	-83.51
 hexanal \rightarrow pentane + CO		-	-70.00
 propionaldehyde \rightarrow C ₂ H ₆ + CO		-	-67.66
 acetaldehyde \rightarrow CH ₄ + CO		-	-78.74
 formaldehyde \rightarrow CH ₄ + CO		-21.09	-50.21
Hydrogenolysis of C-O bond			
 glycerol + H ₂ \rightarrow 1,2-propanediol + H ₂ O		-81.84	-80.58
 glycerol + H ₂ \rightarrow 1,3-propanediol + H ₂ O		-155.50	
 propanol-1 + H ₂ \rightarrow propane + H ₂ O		-81.59	-73.84
 propanol-2 + H ₂ \rightarrow propane + H ₂ O		-77.07	-62.23
 hexanol-2 + H ₂ \rightarrow hexane + H ₂ O		-81.76	-80.29
 hexanol-1 + H ₂ \rightarrow hexane + H ₂ O		-84.43	-95.35
Dehydration			
 glycerol \rightarrow 1-hydroxypropan-2-one + H ₂ O		-	-66.15
 1,2-propanediol \rightarrow acetone + H ₂ O		-103.01	-83.18
 malic acid \rightarrow fumaric acid + H ₂ O		-	9.00
 1,2-ethanediol \rightarrow acetaldehyde + H ₂ O		-90.92	-82.72

Table 2. continued

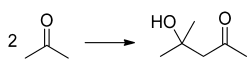
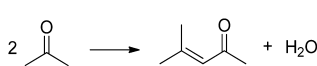
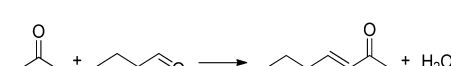

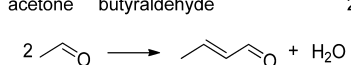
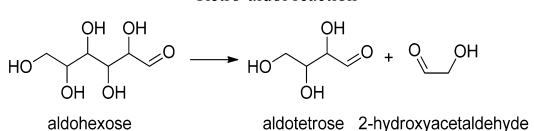
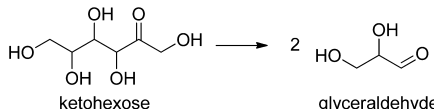
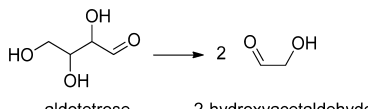
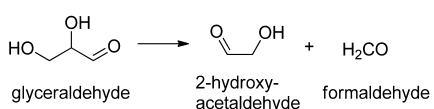
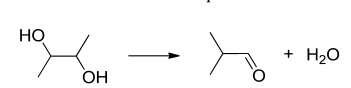
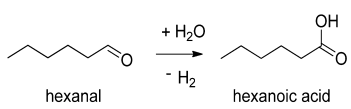
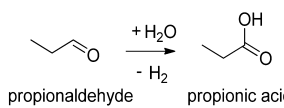
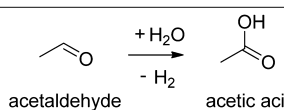
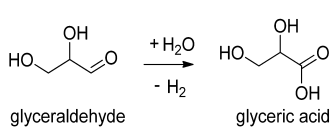
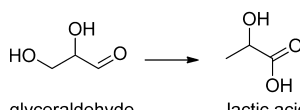
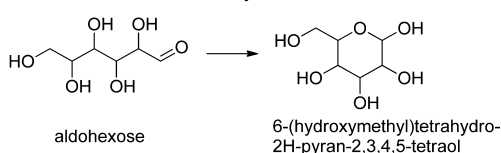
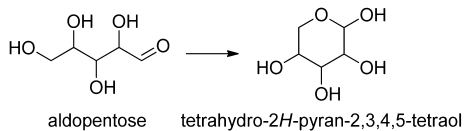
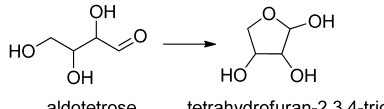
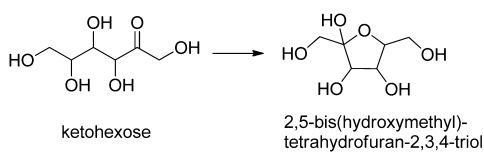
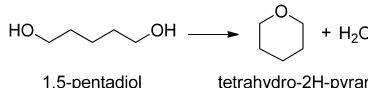
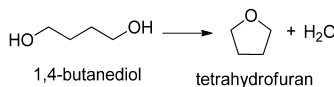
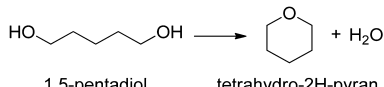
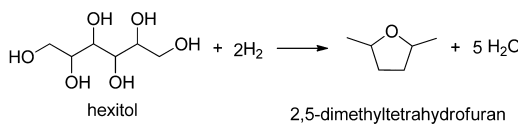
Reaction	Com ment	HyperChem ΔG°_f (498 K) kJ/mol	HSC7 ΔG°_f (498 K) kJ/mol
Aldol condensation			
 acetone → 4-hydroxy-4-methylpentan-2-one		7.49	-36.36
 acetone → 4-methylpent-3-en-2-one + H ₂ O	*	58.70	77.36
 acetone + butyraldehyde → 3-hepten-2-one + H ₂ O	*	28.79	-66.90
 acetone + butyraldehyde + H ₂ → 2-heptenone + H ₂ O		-7.49	-32.80
 2 acetaldehyde → (E)-but-2-enal + H ₂ O		40.29	0.54
Retro-aldol reaction			
 aldohexose → aldotetrose + 2-hydroxyacetaldehyde	*	-72.13	42.84
 ketohexose → 2 glyceraldehyde		-91.09	-
 aldotetrose → 2 2-hydroxyacetaldehyde		-58.07	-
 glyceraldehyde → 2-hydroxyacetaldehyde + H ₂ CO	*	-42.09	-12.97
Pinacol-pinacolone rearrangement			
 2,3-butanediol → isobutyraldehyde + H ₂ O	**	-89.12	-60.33
Formation of acids			
 hexanal + H ₂ O → hexanoic acid - H ₂		3.60	-1.76
 propionaldehyde + H ₂ O → propionic acid - H ₂		-1.38	-38.45

Table 2. continued

Reaction	Com ment	HyperChem ΔG°_f (498 K) kJ/mol	HSC7 ΔG°_f (498 K) kJ/mol
 acetaldehyde → acetic acid		1.38	-7.20
 glyceraldehyde → glyceric acid		341.46	-
 glyceraldehyde → lactic acid	*	175.60	-125.27
Cyclization			
 aldohexose → 6-(hydroxymethyl)tetrahydro-2H-pyran-2,3,4,5-tetraol		14.52	-
 aldopentose → tetrahydro-2H-pyran-2,3,4,5-tetraol		-7.57	-
 aldotetrose → tetrahydrofuran-2,3,4-triol		-13.89	-
 ketohexose → 2,5-bis(hydroxymethyl)-tetrahydrofuran-2,3,4-triol		-24.73	-
 1,5-pentadiol → tetrahydro-2H-pyran + H ₂ O	**	-59.62	-648.02
 1,4-butanediol → tetrahydrofuran + H ₂ O	**	-77.86	-48.74
 1,5-pentadiol → tetrahydro-2H-pyran + H ₂ O		-80.79	-
 hexitol + 2H ₂ → 2,5-dimethyltetrahydrofuran + 5 H ₂ O		-554.17	-353.63

^aLegend: (*) the value of ΔG°_f for one of the substances was calculated in HyperChem; (**); the value of ΔG°_f for one of the substances was taken for a liquid or aqueous phase, according to Table S2 in the Supporting Information.

and acetaldehyde is also thermodynamically favorable (from -67 to -78 kJ/mol), as well as formaldehyde decomposition (-50.21 kJ/mol).

Hydrogenolysis of a C–O bond in an alcohol (path 4 in Figure 14) was assumed to be one of the paths of alkane formation. This reaction was shown to be slightly more favorable

for primary alcohols, such as propan-1-ol and hexan-1-ol, than for corresponding secondary alcohols. Meanwhile, hydrogenolysis of glycerol to propane-1,3-diol is more thermodynamically favorable than that to propane-1,2-diol, indicating a high impact of hydrogen substitution to hydroxyl groups in the adjacent carbon atom. However, the distribution of alcohols in the liquid phase showed zero selectivity to propane-1,3-diol in comparison to 1.4% selectivity to propane-1,2-diol, which can be explained by the higher conversion rates of substances with primary hydroxyl groups. No clear dependence can be found from the distribution of C₄ and C₆ diols and triols, except for the fact that mainly alcohols with adjacent hydroxyl groups were found in the reaction mixture. Thus, probably, in the case of polyols this reaction depends mostly on steric and kinetic factors and is not thermodynamically controlled.

Dehydration reactions were proposed to occur on the acidic sites (path 3 in Figure 14). This reaction is shown to be favorable for glycerol, propane-1,2-diol and ethane-1,2-diol (from -66 to -83 kJ/mol). Formation of fumaric acid, which was found among the products, could be explained by dehydration of malic acid. However, this route is slightly unfavorable (9 kJ/mol).

The next set of reactions is slightly different from the previous one since specific conditions, i.e. the presence of protons and hydroxide ions or Lewis acid (γ -alumina), are required for these reactions.

Aldol condensation was proposed to explain the formation of products with more carbon atoms than are present in the starting material (Figure 19). Unfortunately, only a few examples can be presented in the current study due to the database limitations. The condensation of two molecules of acetone with formation of an aldol is thermodynamically favorable (-36.36 kJ/mol). However, the same reaction combined with subsequent dehydration of the β -hydroxyl group should be unfavorable (the value estimated in HyperChem is 58.7 kJ/mol). The condensation of acetone with butyraldehyde and subsequent dehydrogenation should also be thermodynamically unfavorable (the value estimated in HyperChem is 28.79 kJ/mol). The condensation of two acetaldehydes has a Gibbs energy for the reaction of close to 0. No correlations were found between these calculations and the real product distribution, which indicates that factors other than thermodynamics are responsible for selectivity to different reaction products.

A retro-aldol reaction was proposed to be one of the routes of C–C bond cleavage. Even if the conditions used in the current study do not favor this reaction, some Gibbs energies can be useful. The Gibbs energy of retro-aldol reactions of sugars and glyceraldehyde could only be estimated via quantum-chemical calculations due to the limitations of HSC 7 database, where ΔG°_f values are known only for formaldehyde and glucose. According to HyperChem estimations, the following retro-aldol reactions are thermodynamically favorable: conversion of aldohexose to aldotetrose and 2-hydroxyacetaldehyde (-72.13 kJ/mol) or conversion of ketohexose to glyceraldehydes (-91.09 kJ/mol), conversion of aldotetrose to 2-hydroxyacetaldehydes (-58.07 kJ/mol), conversion of glyceraldehyde to 2-hydroxyacetaldehyde and formaldehyde (-42.09 kJ/mol). These values clearly indicate the possibility of retro-aldol reactions at 225 °C.

The formation of branched alkanes was explained by a pinacol–pinacolone rearrangement (Figure 18), which was shown to be thermodynamically favorable for the conversion of 2,3-butanediol to isobutyraldehyde (-60.33 kJ/mol).

Aldehyde conversion to the intermediate *gem*-diol and the following dehydrogenation was proposed to be the main pathway

of acid formation (Figure 15). The Gibbs energy was shown to be close to 0 for hexanal, propionaldehyde, and acetaldehyde, indicating the possibility of this path for nonsubstituted reactants. At the same time the transformation of glyceraldehyde to glyceric acid is estimated by HyperChem to be highly unfavorable (341.46 kJ/mol).

Another route of acid formation is isomerization of carbonyl compounds with α - and β -hydroxyl groups, which was proposed to occur under the APR conditions by Cortright et al.⁸⁶ However, this mechanism requires rather strongly basic conditions (about 1% Ca(OH)₂)⁸⁸ in comparison to those of the current study. Nevertheless, the Gibbs energy of this reaction at 498 K was shown to be -100.42 kJ/mol;⁷⁸ the value calculated in HSC 7 was -125.27 kJ/mol. An unreliably high positive value appears from HyperChem estimations (175.6 kJ/mol).

The formation of heterocycles can occur by two pathways. The first is cyclization of a carbohydrate-like molecule with a carbon chain length of four to six atoms, where a hydroxyl group reacts with a keto or aldehyde group. Substituted tetrahydrofurans or tetrahydropyrans can be formed via this route. All pentoses and hexoses (both aldehyde and keto forms) are present mostly (>99%) in a cyclic and more thermodynamically favorable form in water solution at 298 K.⁸⁹ Cyclization of ketohexose, aldopentose, and aldotetrose at 498 K is estimated by HyperChem to be slightly thermodynamically favorable (from -7 to -24 kJ/mol), whereas the cyclization of aldohexose is slightly unfavorable (14.52 kJ/mol). The second option is dehydration and intermolecular cyclization. The calculated value by HSC 7 for cyclization of pentane-1,5-diol is -648.02 kJ/mol; however, the value estimated by HyperChem is approximately 10 times lower (-59.62 kJ/mol). The reason for this discrepancy might be an inaccuracy in the calculation of ΔG°_f for tetrahydropyran in HSC 7.0. The cyclization of butane-1,4-diol is thermodynamically favorable (values calculated by HSC 7 and estimated by HyperChem are -48.74 and -77.86 kJ/mol, respectively). The cyclization of hexane-2,5-diol is estimated by HyperChem to be thermodynamically favorable (-80.79 kJ/mol). The formation of 2,5-dimethyltetrahydrofuran via cyclization of hexitol and subsequent hydrogenolysis is also thermodynamically favorable (the HSC 7 value is -353.17 kJ/mol, while that estimated in HyperChem is -554.17 kJ/mol).

4. CONCLUSIONS

The difference in reactivity of two naturally abundant sugar alcohols in the APR, galactitol and sorbitol, was studied over a stable Pt/Al₂O₃ catalyst at 225 °C. Gas and liquid products were thoroughly studied by means of GC and HPLC analysis, with the carbon balance being close to 90–95%. It was observed that the conversion levels were very similar for both substrates and their mixture. The gas-phase composition was also similar, in contrast to the liquid-phase product distribution with minor, but noticeable, differences for some intermediates, such as acids (tartaric, pyruvic, and fumaric), carbohydrates (glucose and galactose), and polyols (arabitol and xylitol). The liquid-phase compositions for both compounds were elucidated with a very high degree of product identification: up to 80%. The reliability of identification was significantly improved due to the introduction of a spiking technique and peak fitting. The high precision of product identification was important, allowing us to introduce possible reaction mechanisms in accord with to the product distribution. Diastereomerization of carbohydrates was proposed to explain the formation of both glucose and galactose from sorbitol, and the differences in selectivities to some primary

intermediates (xylitol, arabinol, glucose, and galactose). Heptane formation was explained via aldol and croton condensation. Additionally, reaction pathways were discussed from a thermodynamic point of view. The Gibbs reaction energy was found to be close to 0 for dehydrogenation reactions. Hydrogenolysis of the C–O bond and decarbonylation were shown to be thermodynamically favorable for most reactants.

It was shown that during the initial stages of the APR reaction sorbitol and galactitol generally generated similar primary intermediates, even if they were not exactly the same. Selectivities to the final products, such as hydrogen, CO₂, and alkanes, were essentially the same. Therefore, substrates with different chiralities, as well as their mixtures, can be used in the APR for production of hydrogen and/or alkanes.

■ ASSOCIATED CONTENT

Supporting Information

The following file is available free of charge on the ACS Publications website at DOI: 10.1021/cs501894e.

The free Gibbs energy values of feasible products and intermediates calculated in HSC 7 Chemistry and estimated in HyperChem programs ([PDF](#))

■ AUTHOR INFORMATION

Corresponding Author

*E-mail for D.Y.M.: dmurzin@abo.fi.

Present Address

[†](A.V.K.) Dow Benelux BV, P.O. Box 48, Building 443, 4530 AA Terneuzen, The Netherlands.

Notes

The authors declare no competing financial interest.

■ ACKNOWLEDGMENTS

The SusFuelCat project has received funding from the European Union's Seventh Framework Programme for research, technological development and demonstration under Grant Agreement No. 310490 (www.susfuelcat.eu). The authors gratefully thank M.Sc. Yury Brusentsev and Dr. Denis Mavrinskiy from the Laboratory of Organic Chemistry, Åbo Akademi University, and Dr. Yulia Demidova from the Boreskov Institute of Catalysis for valuable discussions during manuscript preparation. We acknowledge the Laboratory of Wood and Paper Chemistry, Åbo Akademi University, for technical support.

■ REFERENCES

- (1) Davda, R. R.; Shabaker, J. W.; Huber, G. W.; Cortright, R. D.; Dumesic, J. A. *Appl. Catal., B* **2005**, *56*, 171–186.
- (2) Liu, B. *Catalytic Generation of Hydrogen and Chemicals from Biomass Derived Polyols*; ProQuest: Ann Arbor, MI, 2008; p 159.
- (3) He, L.; Chen, D. *ChemSusChem* **2012**, *5*, 587–595.
- (4) Tanksale, A.; Beltramini, J. N.; Lu, G. M. *Renewable Sustainable Energy Rev.* **2010**, *14*, 166–182.
- (5) Vilcoq, L.; Cabiac, A.; Especel, C.; Guillon, E.; Duprez, D. *Oil Gas Sci. Technol.* **2013**, *68*, 841–860.
- (6) Wei, Y.; Lei, H.; Liu, Y.; Wang, L.; Zhu, L.; Zhang, X.; Yadavalli, G.; Ahring, B.; Chen, S. *J. Sustainable Bioenergy Syst.* **2014**, *4*, 113–127.
- (7) Hoffer, B. W.; Crezee, E.; Devred, F.; Mooijman, P. R. M.; Sloof, W. G.; Kooyman, P. J.; van Langeveld, A. D.; Kapteijn, F.; Moulijn, J. A. *Appl. Catal., A* **2003**, *253*, 437–452.
- (8) Crezee, E.; Hoffer, B. W.; Berger, R. J.; Makkee, M.; Kapteijn, F.; Moulijn, J. A. *Appl. Catal., A* **2003**, *251*, 1–17.
- (9) van Gorp, K.; Boerman, E.; Cavenaghi, C. V.; Berben, P. H. *Catal. Today* **1999**, *52*, 349–361.
- (10) Jaime, W.; Rozita, S. *Ind. Eng. Chem. Prod. Res. Dev.* **1979**, *18*, 50–57.
- (11) Kusserow, B.; Schimpf, S.; Claus, P. *Adv. Synth. Catal.* **2003**, *345*, 289–299.
- (12) Perrard, A.; Gallezot, P.; Joly, J.-P.; Durand, R.; Baljou, C.; Coq, B.; Trems, P. *Appl. Catal., A* **2007**, *331*, 100–104.
- (13) Wen, J.-P.; Wang, C.-L.; Liu, Y.-X. *J. Chem. Technol. Biotechnol.* **2004**, *79*, 403–406.
- (14) Deng, W.; Tan, X.; Fang, W.; Zhang, Q.; Wang, Y. *Catal. Lett.* **2009**, *133*, 167–174.
- (15) Han, J. W.; Lee, H. *Catal. Commun.* **2012**, *19*, 115–118.
- (16) Liu, M.; Deng, W.; Zhang, Q.; Wang, Y.; Wang, Y. *Chem. Commun. (Cambridge, U. K.)* **2011**, *47*, 9717–9719.
- (17) Negoi, A.; Triantafyllidis, K.; Parvulescu, V. I.; Coman, S. M. *Catal. Today* **2014**, *223*, 122–128.
- (18) Xi, J.; Zhang, Y.; Xia, Q.; Liu, X.; Ren, J.; Lu, G.; Wang, Y. *Appl. Catal., A* **2013**, *459*, 52–58.
- (19) Zhang, J.; Wu, S.; Liu, Y. *Energy Fuels* **2014**, *28*, 4242–4246.
- (20) Wang, D.; Niu, W.; Tan, M.; Wu, M.; Zheng, X.; Li, Y.; Tsubaki, N. *ChemSusChem* **2014**, *1398*–1406.
- (21) Käldestrom, M.; Kumar, N.; Murzin, D. Y. *Catal. Today* **2011**, *167*, 91–95.
- (22) Chen, J.; Wang, S.; Huang, J.; Chen, L.; Ma, L.; Huang, X. *ChemSusChem* **2013**, *6*, 1545–1555.
- (23) Fukuoka, A.; Dhepe, P. L. *Angew. Chem.* **2006**, *118*, 5285–5287.
- (24) Willför, S.; Rehn, P.; Sundberg, A.; Sundberg, K.; Holmbom, B. *Tappi J.* **2003**, *2*, 27–32.
- (25) Sjöström, E. *Wood Chemistry Fundamentals and Applications*, 2nd ed.; Gulf Professional Publishing, Nature: Helsinki University of Technology: Espoo, Finland, 1993; p 293.
- (26) Kusema, B. T.; Tönnov, T.; Mäki-Arvela, P.; Salmi, T.; Willför, S.; Holmbom, B.; Murzin, D. Y. *Catal. Sci. Technol.* **2013**, *3*, 116.
- (27) Xu, C.; Pranovich, A.; Vähäsalo, L.; Hemming, J.; Holmbom, B.; Schols, H. A.; Willför, S. *J. Agric. Food Chem.* **2008**, *56*, 2429–2435.
- (28) Deutsch, K. L.; Lahr, D. G.; Shanks, B. H. *Green Chem.* **2012**, *14*, 1635.
- (29) Kirilin, A. V.; Tokarev, A. V.; Kustov, L. M.; Salmi, T.; Mikkola, J.; Murzin, D. Y. *Appl. Catal., A* **2012**, *435*–436, 172–180.
- (30) Li, N.; Huber, G. W. *J. Catal.* **2010**, *270*, 48–59.
- (31) Moreno, B. M.; Li, N.; Lee, J.; Huber, G. W.; Klein, M. T. *RSC Adv.* **2013**, *3*, 23769–23784.
- (32) Vilcoq, L.; Cabiac, A.; Especel, C.; Lacombe, S.; Duprez, D. *J. Catal.* **2014**, *320*, 16–25.
- (33) Vilcoq, L.; Cabiac, A.; Especel, C.; Lacombe, S.; Duprez, D. *Catal. Today* **2015**, *242*, 91–100.
- (34) Jin, X.; Subramaniam, B.; Chaudhari, R. V. In *Novel Materials for Catalysis and Fuels Processing*; American Chemical Society: Washington, DC, 2013; ACS Symposium Series 1132, pp 273–285.
- (35) Aiouache, F.; McAleer, L.; Gan, Q.; Al-Muhtaseb, A. H.; Ahmad, M. N. *Appl. Catal., A* **2013**, *466*, 240–255.
- (36) Kirilin, A. V.; Tokarev, A. V.; Murzina, E. V.; Kustov, L. M.; Mikkola, J.-P.; Murzin, D. Y.; Aqueous. *ChemSusChem* **2010**, *3*, 708–718.
- (37) *OriginPro 9.0.0*; OriginLab Corporation, Northampton, MA, USA, 2012.
- (38) Yao, H. C.; Sieg, M.; Plummer, H. K. *J. Catal.* **1979**, *59*, 365–374.
- (39) Otter, G. J. den; Dautzenberg, F. M. *J. Catal.* **1978**, *53*, 116–125.
- (40) Barbelli, M. L.; Pompeo, F.; Santori, G. F.; Nichio, N. N. *Catal. Today* **2013**, *213*, 58–64.
- (41) Copeland, J. R.; Foo, G. S.; Harrison, L. A.; Sievers, C. *Catal. Today* **2013**, *205*, 49–59.
- (42) El Doukkali, M.; Iriondo, A.; Arias, P. L.; Requies, J.; Gandarias, I.; Jalowiecki-Duhamel, L.; Dumeignil, F. *Appl. Catal., B* **2012**, *125*, 516–529.
- (43) El Doukkali, M.; Iriondo, A.; Cambra, J. F.; Gandarias, I.; Jalowiecki-Duhamel, L.; Dumeignil, F.; Arias, P. L. *Appl. Catal., A* **2014**, *472*, 80–91.
- (44) He, R.; Davda, R. R.; Dumesic, J. A. *J. Phys. Chem. B* **2005**, *109*, 2810–2820.

- (45) Iriondo, A.; Barrio, V. L.; Cambra, J. F.; Arias, P. L.; Güemez, M. B.; Navarro, R. M.; Sánchez-Sánchez, M. C.; Fierro, J. L. G. *Top. Catal.* **2008**, *49*, 46–58.
- (46) Menezes, A. O.; Rodrigues, M. T.; Zimmaro, A.; Borges, L. E. P.; Fraga, M. A. *Renewable Energy* **2011**, *36*, 595–599.
- (47) Peng, B.; Zhao, C.; Mejía-Centeno, L.; Fuentes, G. A.; Jentys, A.; Lercher, J. A. *Catal. Today* **2012**, *183*, 3–9.
- (48) Ravenelle, R. M.; Copeland, J. R.; Pelt, A. H.; Crittenden, J. C.; Sievers, C. *Top. Catal.* **2012**, *55*, 162–174.
- (49) Roy, B.; Loganathan, K.; Pham, H. N.; Datye, A. K.; Leclerc, C. A. *Int. J. Hydrogen Energy* **2010**, *35*, 11700–11708.
- (50) Wawrzetz, A.; Peng, B.; Hrabar, A.; Jentys, A.; Lemonidou, A. A.; Lercher, J. A. *J. Catal.* **2010**, *269*, 411–420.
- (51) Doukkali, M. El; Iriondo, A.; Cambra, J. F.; Gandarias, I.; Jalowiecki-duhamel, L.; Dumeignil, F.; Arias, P. L. *Appl. Catal., A* **2014**, *472*, 80–91.
- (52) Sakurai, H.; Ueda, A.; Kobayashi, T.; Haruta, M. *Chem. Commun.* **1997**, 271–272.
- (53) Meadhra, R. Ó.; Lin, R. *Chem. Eng. Res. Des.* **2006**, *84*, 711–720.
- (54) Miljkovic, M. *Carbohydrates: Synthesis, Mechanisms, and Stereo-electronic Effects*; Springer: Heidelberg, Germany, 2009; p 543.
- (55) Li, N.; Tompsett, G. A.; Zhang, T.; Shi, J.; Wyman, C. E.; Huber, G. W. *Green Chem.* **2011**, *13*, 91–101.
- (56) Auneau, F.; Noël, S.; Aubert, G.; Besson, M.; Djakovitch, L.; Pinel, C. *Catal. Commun.* **2011**, *16*, 144–149.
- (57) Zhang, J.; Lu, F.; Yu, W.; Chen, J.; Chen, S.; Gao, J.; Xu, J. *Catal. Today* **2014**, *234*, 107–112.
- (58) Roy, D.; Subramaniam, B.; Chaudhari, R. V. *Catal. Today* **2010**, *156*, 31–37.
- (59) Gandarias, I.; Arias, P. L.; Requies, J.; Güemez, M. B.; Fierro, J. L. G. *Appl. Catal., B* **2010**, *97*, 248–256.
- (60) Smith, M. B. *March's advanced organic chemistry reactions, mechanisms and structure*, 7th ed.; Wiley: Hoboken, NJ, 2013; p 2080.
- (61) Parvulescu, A.; Janssens, J.; Vanderleyden, J.; Vos, D. *Top. Catal.* **2010**, *53*, 931–941.
- (62) Nishimura, S.; Yakita, Y.; Katayama, M.; Higashimine, K.; Ebitani, K. *Catal. Sci. Technol.* **2013**, *3*, 351–359.
- (63) Kim, W.; Karvembu, R.; Park, J. *Bull. Korean Chem. Soc.* **2004**, *25*, 931–933.
- (64) Shi, J.; Li, X.; Wang, Q.; Zhang, Y.; Tang, Y. *J. Catal.* **2012**, *291*, 87–94.
- (65) Martín-Matute, B.; Bäckvall, J.-E. *Curr. Opin. Chem. Biol.* **2007**, *11*, 226–232.
- (66) Bandura, A. V.; Lvov, S. N. *J. Phys. Chem. Ref. Data* **2006**, *35*, 15–30.
- (67) Banu, M.; Sivasanker, S.; Sankaranarayanan, T. M.; Venuvalingam, P. *Catal. Commun.* **2011**, *12*, 673–677.
- (68) Clark, I. *Ind. Eng. Chem.* **1958**, *50*, 1125–1126.
- (69) Zhao, L.; Zhou, J. H.; Sui, Z. J.; Zhou, X. G. *Chem. Eng. Sci.* **2010**, *65*, 30–35.
- (70) Sun, J.; Liu, H. *Green Chem.* **2011**, *13*, 135–142.
- (71) Jiang, T.; Wang, T.; Ma, L.; Li, Y.; Zhang, Q.; Zhang, X. *Appl. Energy* **2012**, *90*, 51–57.
- (72) Guo, Y.; Azmat, M. U.; Liu, X.; Wang, Y.; Lu, G. *Appl. Energy* **2012**, *92*, 218–223.
- (73) Ciftci, A.; Ligthart, D. A. J. M.; Sen, A. O.; van Hoof, A. J. F.; Friedrich, H.; Hensen, E. J. M. *J. Catal.* **2014**, *311*, 88–101.
- (74) Ciftci, A.; Ligthart, D. A. J. M.; Hensen, E. J. M. *Green Chem.* **2014**, *16*, 853.
- (75) Huber, G. W.; Cortright, R. D.; Dumesic, J. A. *Angew. Chem., Int. Ed.* **2004**, *43*, 1549–1551.
- (76) Zhang, Q.; Qiu, K.; Li, B.; Jiang, T.; Zhang, X.; Ma, L.; Wang, T. *Fuel* **2011**, *90*, 3468–3472.
- (77) Zhang, Q.; Wang, T.; Li, B.; Jiang, T.; Ma, L.; Zhang, X.; Liu, Q. *Appl. Energy* **2012**, *97*, 509–513.
- (78) Simonetti, D. A.; Dumesic, J. A. *Catal. Rev.: Sci. Eng.* **2009**, *51*, 441–484.
- (79) Kandoi, S.; Greeley, J.; Simonetti, D.; Shabaker, J.; Dumesic, J. A.; Mavrikakis, M. *J. Phys. Chem. C* **2011**, *115*, 961–971.
- (80) Xie, J.; Su, D.; Yin, X.; Wu, C.; Zhu, J. *Int. J. Hydrogen Energy* **2011**, *36*, 15561–15572.
- (81) Luo, N.; Zhao, X.; Cao, F.; Xiao, T.; Fang, D. *Energy Fuels* **2007**, *21*, 3505–3512.
- (82) Luo, N.; Cao, F.; Zhao, X.; Xiao, T.; Fang, D. *Fuel* **2007**, *86*, 1727–1736.
- (83) Jun, J.-W.; Suh, Y.-W.; Suh, D. J.; Lee, Y.-K. *J. Ind. Eng. Chem.* **2013**, *19*, 2072–2078.
- (84) *HSC Chemistry 6.0*, Outotec Oy, Espoo, Finland, 2006.
- (85) *HyperChem Pro 8.0.8*; Hypercube, Inc., Gainesville, FL, USA, 2009.
- (86) Cortright, R. D.; Davda, R. R.; Dumesic, J. A. *Nature* **2002**, *418*, 964–967.
- (87) Liu, J.; Chu, X.; Zhu, L.; Hu, J.; Dai, R.; Xie, S.; Pei, Y.; Yan, S.; Qiao, M.; Fan, K. *ChemSusChem* **2010**, *3*, 803–806.
- (88) Collins, P. M.; Ferrier, R. J. *Monosaccharides: Their Chemistry and Their Roles in Natural Products*, 1st ed.; Wiley: New York, 1995; p 587.
- (89) Goldberg, R. N.; Tewari, Y. B. *J. Phys. Chem. Ref. Data* **1989**, *18*, 809–880.